Memoirs of the Faculty of Engineering, Nagoya University
Vol. 40, No. 2 (1988) – Research Report –

AN APPLICATION OF THE SURFACE-SINGULARITY METHOD TO WING-BODY-TAIL CONFIGURATIONS

JANG-SOO CHOI, KEUN-SHIK CHANG* and YOSHIYUKI SUGIYAMA

Department of Aeronautical Engineering

(Received October 31, 1988)

Abstract

A computer code based on the 1st order panel method is presented for solving inviscid incompressible flow fields about 3-D airplane-like bodies. A sample problem chosen for a test is solved and a comparison with other computational results shows good agreement. To increase the accuracy of the method, especially for a thin wing, the number of doublet panels on the camber surface of a wing is multiplied in the chordwise direction by a factor, which enhances the accuracy to some extent.

1. Introduction

The incompressible potential flow fields whose governing equation is Laplace's differential equation have been able to be solved effectively even in the case of complicated boundary conditions such as airplane-like bodies, owing to the rapid development of computers and numerical methods. The most effective method for such a problem has been known to be the panel method, that is, the surface-singularity method or the boundary element method, which is being, nowadays, used widely in the field of airplane design because of its usefulness. This surface-singularity method is superior to the other methods such as FDM or FEM, because the surface-singularity method can solve such problems as mentioned above more economically, with its unknowns placed only on the body surface, not on the whole flow field as in FDM or FEM.

* Department of Mechanical Engineering, Korea Advanced Institute of Science and Technology, Korea

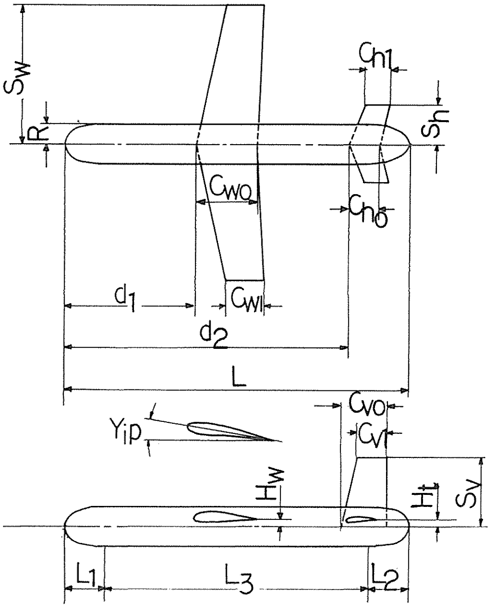

(Cylindrical fuselage length)

Fig. 1. Airplane geometry treated in program

In this paper a computer code which is able to solve a flow about the configuration as shown in Fig. 1 with the panel method is presented. In fact, it is not so simple to define a body surface with an arbitrary complicated configuration that the application of the code is confined to a body of the configuration consisting of an axisymmetric fuselage, a wing and a tail which have an arbitrary wing section, aspect ratio, sweep angle and attachment angle. The geometrical parameters needed for the present code are also shown in Fig. 1.

To show the accuracy of the code, a wing-only problem has been solved. A comparison with known numerical results shows good agreement.

2. Derivation of Integral Equation

For an irrotational incompressible flow field the velocity potential Φ satisfies Laplace's equation:

$$\nabla^2\Phi=0 \tag{1}$$

upon which the panel method relies. If we consider a body at rest in a uniform flow, the boundary conditions will be given as follows:

$$\frac{\partial \Phi}{\partial n}=0 \tag{2}$$

on the body surface if the surface is impermeable, and

$$\nabla \Phi=\vec{V}_{\infty}$$

at infinity.

It is possible to transform equation (1) into a variety of the equivalent integral form by Green's integral formula.

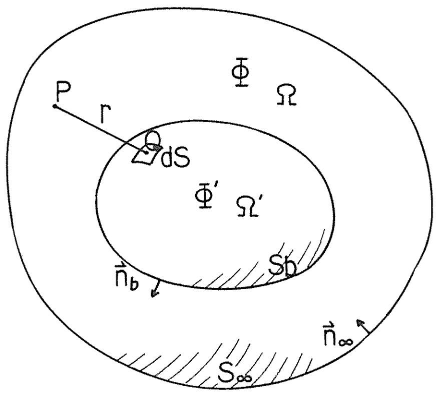

Fig. 2. Mathematical modeling of flow field

Consider a domain Ω enclosed by the closed surfaces S_{∞} and S_b (*see Fig. 2*) and assume that a velocity potential which satisfies equation (1) is defined both in the domain and on the surfaces; the local normals to the surfaces are respectively $\vec{n}_{\infty}$ and $\vec{n}_b$, directed as shown in Fig. 2, then Green's formula says:

$$\begin{aligned} 4\pi H\Phi_p=&\oiint_{S_\infty}\left[-\frac{1}{r}\vec{n}_\infty\cdot\nabla\Phi+\Phi\,\vec{n}_\infty\cdot\nabla\left(\frac{1}{r}\right)\right]dS \\ &+\oiint_{S_b}\left[-\frac{1}{r}\vec{n}_b\cdot\nabla\Phi+\Phi\,\vec{n}_b\cdot\nabla\left(\frac{1}{r}\right)\right]dS \end{aligned} \tag{3}$$

where the subscript p denotes a fixed point P lying inside Ω or on the boundary S_b, r is defined to be the length of the vector $\vec{r}$ drawn from the surface element dS lying on S_b

and S_∞ to P, H is a value determined according to the position P lies, i.e. $H=1$ when P lies inside Ω, $H=1/2$ when on the smooth surface of S_b, and the integral symbol $\oiint$ means the integration excludes the singular point at which P coincides with a point Q lying on the surface of integration ($r=0$). The first integral on the right-hand side of equation (3) means the undisturbed potential at P and is written as $4\pi\Phi_{\infty p}$. This equation, when $H=1/2$, may be directly utilized to obtain one of Φ and $\frac{\partial \Phi}{\partial n}$, if only the other one of the two values is known on the boundary, after that, it is possible to get the value of Φ at all points in the domain Ω by the same equation (for values on S_b $H=1/2$, for values inside Ω $H=1$).

Alternative integral forms, however, may be derived[1]. Now if we define another fictitious potential Φ' in the domain Ω' enclosed by the surface S_b, again applying Green's formula in the case where the point P lies outside Ω', we obtain:

$$0=\oiint_{S_b} [-\frac{1}{r}(-\vec{n}_b)\cdot\nabla\Phi'+\Phi'(-\vec{n}_b)\cdot\nabla(\frac{1}{r})]\mathrm{d}S \tag{4}$$

Adding equation (4) to equation (3), we have:

$$4\pi H\Phi_p=4\pi\Phi_{\infty p}+\oiint_{S_b} [-\frac{1}{r}\vec{n}_b\cdot(\nabla\Phi-\nabla\Phi')+(\Phi-\Phi')\vec{n}_b\cdot\nabla(\frac{1}{r})]\mathrm{d}S \tag{5}$$

In a practical problem we have an interest only in the outer domain Ω and are given boundary conditions in the domain only, so that if equation (5) is to be determinate for such a problem, an assumption of the boundary conditions on the inner side of the boundary S_b is necessary. This arbitrariness to choose the potential Φ' in the inner domain Ω' may be, if with good skill of choice, exploited to make the problem easy to solve with efficiency and small error numerically.

It may be shown that the integral on the right-hand side of equation (5) can be interpreted as the potential caused by a surface source of variable density σ and a surface doublet of variable density μ with the doublet axis coinciding with $\vec{n}_b$, if we equate:

$$\sigma=\vec{n}_b\cdot(\nabla\Phi-\nabla\Phi')\ ,\ \mu=-(\Phi-\Phi')$$

Then, equation (5) may be written for an arbitrary point P not lying on the boundary S_b:

$$4\pi\Phi_p=4\pi\Phi_{\infty p}+\iint_{S_b}[-\frac{\sigma}{r}-\mu\,\vec{n}_b\cdot\nabla(\frac{1}{r})]\mathrm{d}S \tag{6}$$

For a point P lying on S_b the same equation may be used, provided the integral is defined to include the local singular contribution $-2\pi\mu_p$ due to the local doublet density μ_p. By applying the operator ∇_P to both sides of equation (6) we get the following expression about the velocity $\vec{V}_p$ at P:

$$4\pi\vec{V}_p=4\pi\vec{V}_{\infty p}+\iint_{S_b}[-\sigma\nabla_p(\frac{1}{r})-\mu\nabla_p(\vec{n}_b\cdot\nabla(\frac{1}{r}))]\mathrm{d}S \tag{7}$$

About equations (6) and (7) the equivalent statement as in equation (5) may be made, i.e. to render the equations determinate, it is necessary to assume one of two unknowns, σ and μ on S_b. It means that an infinite number of different combinations of σ and μ distributions may exist for the same boundary conditions given on the outer surface only. We should, therefore, determine the distribution which not only satisfies the boundary condition, but which also minimizes the numerical errors in that domain.

In the ideal fluid the wake behind a wing is idealized as an infinitely thin sheet of discontinuity, on which surface doublet is laid. Even though the position and the configuration of the wake is not known beforehand but determined by the calculation of the flow field, it is assumed that the wake lies at a fixed position since the influence of its spatial variation on the flow around the wing may be neglected. Because of some numerical reasons surface doublet is laid not only on the wake, but also on the upper surface or the camber surface of the wing, as shown in Fig. 3. In the case where we lay doublet only on the wake, because the influence induced on the Kutta points near the trailing edge by the doublet becomes much larger than that of the source distribution on the wing, the application of the Kutta condition to the Kutta points brings about the vanishing of surface doublet density. Consequently, the problem reduces to a source-only-distributed problem without lift.

The doublet distribution on the extended surface in the wing is expressed as a mode function $\phi(\xi)$ in the chordwise direction together with an unknown magnitude factor μ_k. Thus,

$$\mu=\mu_k\phi(\xi) \tag{8}$$

Theoretically the Kutta condition is stated as the avoidance of an infinite velocity at the trailing edge. Such a condition, however, cannot be enforced numerically. Hence we place the Kutta points a short distance (about 1/3% of local chord) downstream of the trailing edge on its extended camber surface and apply the condition that the component of the velocity normal to the surface at these points vanishes.

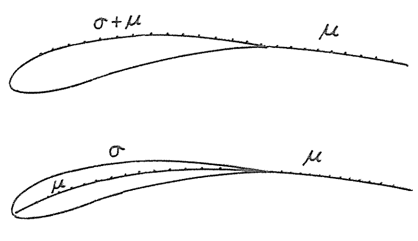

Fig. 3. Surface doublet extended into wing

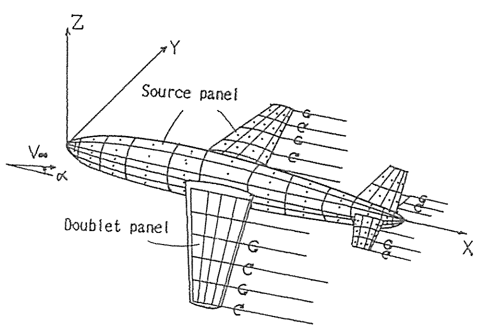

Fig. 4. Distribution of singularities over airplane

In the present code, on the body surface is laid a surface source, while on the camber surfaces and wakes of a wing and tail is laid a surface doublet, as shown in Fig. 4. If we apply the boundary condition of (2) to equation (7), we have the following:

$$0=4\pi \vec{V}_\infty \cdot \vec{n}_p+\iint_{S_o} (-\sigma \vec{n}_p \cdot \nabla_p(\frac{1}{r})) dS+\iint_{S_w} -\mu \vec{n}_p \cdot \nabla_p(\vec{n} \cdot \nabla(\frac{1}{r})) dS \quad (9)$$

where S_o expresses the surface of an airplane shown in Fig. 4, S_w means the camber surface and the wake of the wing, and the first integral on the right-hand side of the equation is defined to include the local singular contribution $2\pi\sigma_p\vec{n}_p$ due to the local source density σ_p.

3. Numerical Formulation

3. 1. *Discretization*

To solve equation (9), it is necessary to discretize properly the body surface, the distribution of surface singularities, and the boundary condition. There can exist various methods of discretization, for example, on each panel of the body surface a simple plane or spline representation may be used, while the surface singularity distribution may be represented by one of discrete, linear or curvilinear variations. The present code adopts the 1st order method which has been widely used because of its simplicity to calculate the influence coefficients. It is written as follows.

(1) The body surface is represented by a lot of plane panels made by every 4 points on the surface.

(2) On every panel a singularity of constant density is distributed.

(3) The boundary condition is applied to every control point which is the centroid of a panel.

If we represent the plane panel of the surface as a subscript j and the control point as a subscript i, dividing the integral region of the equation (9) into panels, then for the control point i, we have:

$$\sum_j X_j \vec{n}_i \cdot \vec{C}_{ij}+\sum_k X_k \vec{n}_i \cdot \vec{C}_{ik}=-\frac{\vec{V}_\infty}{V_\infty} \cdot \vec{n}_i \quad (10)$$

where

$$\vec{C}_{ij}=\iint_{\substack{\text{panel}\\ j}} - \nabla_p(\frac{1}{r}) dS \quad , \quad \vec{C}_{ik}= \iint_{\substack{\text{doublet}\\ \text{strip } k}} -\phi \left[\nabla_p(\vec{n} \cdot \nabla (\frac{1}{r})) \right] dS$$

$$X_j=\frac{\sigma_j}{4\pi V_\infty} \quad , \quad X_k=\frac{\mu_k}{4\pi V_\infty}$$

The influence vector $\vec{C}_{ij}$ means the velocity induced at a control point i by a panel j on which surface source of unit density lies and $\vec{C}_{ik}$ represents the velocity induced at the same control point i by a wing strip k with doublet distribution of $\phi(\xi)$.

3. 2. Calculation of influence vectors

$\vec{C}_{ik}$ is calculated by the Gaussian integral (*see Appendix*), where the number of Gaussian points varies according to the distance between the control point and the panel. For the control point sufficiently long distance, the formula of a point source is used. According to the equivalence law obtained by B. Hunt[1)], a panel with a constant density as in the present paper can be transformed into a ring vortex around the perimeter of the panel, therefore, its influence is calculated easily by Viot-Savart's law. $\vec{C}_{ik}$ is calculated by adding all the influence induced by every doublet panel of wing strip k to the influence induced by the trailing vortex of that strip.

3. 3. Formation of the linear equation system

If we let $\vec{n}_i \cdot \vec{C}_{ij} = A_{ij}$, $\vec{n}_i \cdot \vec{C}_{ik} = A_{ik}$, *and* $-(\vec{V}_\infty / V_\infty) \cdot \vec{n}_i = B_i$, equation (10) is rewritten as:

$$\sum_j A_{ij} X_j + \sum_k A_{ik} X_k = B_i$$

In a matrix form, it is expressed as $\boldsymbol{AX}=\boldsymbol{B}$. If the body is symmetric about the plane $y=0$ and the oncoming flow is likewise symmetric, the resulting singularity density must also be symmetric. In such a case, the number of matrix elements may thus be reduced by a factor of 4 (though the number of unknowns is halved), by adding up the two influences induced by each pair of panels. Boundary conditions are then applied only to half control points on the right-hand side of the xz-plane.

The solution of the linear equation system may be efficiently obtained by iteration method because the matrix $\boldsymbol{A}$ has the largest value in the diagonal elements. Due to linearity of the equation, the solutions for various angles of incidence can be obtained by the linear combination of the two basic solutions for $\alpha=0°$ and $90°$. This is because, even though the angle of incidence of the oncoming flow varies, the matrix $\boldsymbol{A}$ not changing, the column vector $\boldsymbol{B}$ only becomes different. If we suppose the column vectors for $\alpha=0°$ and $90°$ are $\boldsymbol{B}_1$ and $\boldsymbol{B}_2$ respectively, the column vector $\boldsymbol{B}$ for an arbitrary α becomes $\cos\alpha \cdot \boldsymbol{B}_1 + \sin\alpha \cdot \boldsymbol{B}_2$. It can be concluded that the solution $\boldsymbol{X}$ for α is obtained by the relation

$$X = \cos\alpha \cdot X_1 + \sin\alpha \cdot X_2$$

where $\boldsymbol{X}_1$ and $\boldsymbol{X}_2$ are the solutions for $\alpha=0°$ and $90°$, that is, the solutions of the equations $\boldsymbol{AX}=\boldsymbol{B}_1$, $\boldsymbol{AX}=\boldsymbol{B}_2$, respectively.

4. Verification of the Present Code for a Simple Wing Configuration

4. 1. Adoption of a model problem

To estimate the numerical accuracy of a code based on the panel method, the computational result is compared, not with experimental data directly, but with a theoretical solution or more exact solution of the governing equation, that is, a solution obtained by a higher order method. Such a comparison may determine whether both the method used and the code are accurate or not.

As shown in Fig. 5, a model problem is about a simple sweptback tapered wing. Thus, a wing-only problem is chosen, with a fuselage and a tail wing omitted from Fig. 1 for simplicity. It is one of the model problems adopted by some relevant researchers to try to establish some standard solutions of them for the estimation of various panel

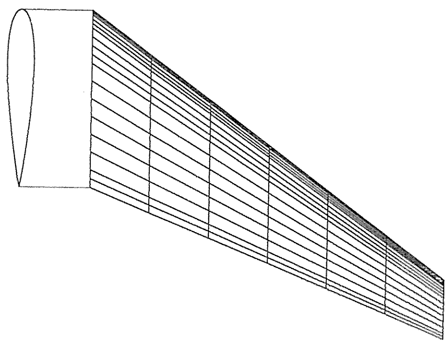

Fig. 5. Planform of tapered sweptback wing (RAE Wing A; Wing section NACA 0015) and its discretization

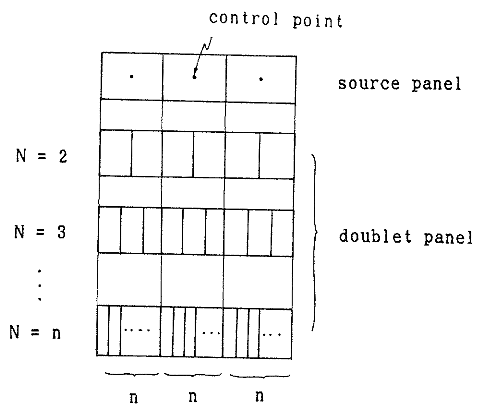

Fig. 6. Increase of doublet panels

methods. The form of the wing is the planform, RAE Wing A, and its airfoils are symmetric NACA 4-digit sections with the thickness ratio of 0.05 and 0.15.

The wing surface has 36 source panels per each wing strip (18 panels on the upper and lower surfaces) on 6 wing strips on the half wing, as shown in Fig. 5. The number of doublet panels on camber surface is, usually, the same as that of source panels on the upper surface of the wing. As shown by J. Ballmann, et al.[3], a numerical model of a doublet distribution should have one degree higher continuity than that of a source distribution for an equivalent order of error between both distributions, i.e. a constant distribution of source on a panel is compatible with a linear distribution of doublet on a panel (the so-called 'sheets model'). In the present code, however, is used a constant distribution of doublet on a panel, which is termed the 'lines model'.

For a remedy for this situation, the number of doublet panels is multiplied by a factor in the chordwise direction in such a way as shown in Fig. 6, in the present code.

4. 2 Numerical results and discussion

Fig. 7 shows, at no lift, the comparison of C_p distribution on a wing section, $\eta=0.55$ between A. Roberts' result[1] and the present one. The present results were obtained for the discretization, $I \times J=36\times6$ and 72×6, where I is the number of panels per wing strip consisting of upper and lower surfaces, and J the number of wing strips per half wing. Roberts' solution is that obtained by a higher order panel method. The comparison shows good agreement with Roberts' in both cases of I. The spanwise lift distribution $(1/2)c\cdot C_l(\xi)$, determined by numerically integrating the computed pressure distribution, is shown in Figs. 8(*a*) and (*b*) for $t/c=0.05$ and 0.15, respectively, at $\alpha=5°$, together with the effect of the multiplying factor N. Although the result for $t/c = 0.15$ is nearly the same as Hunt's, which was obtained with 'sheets model', considerable error for $t/c=0.05$ is demonstrated. It may be, therefore, said that 'lines model' produces marked error for a very thin wing.

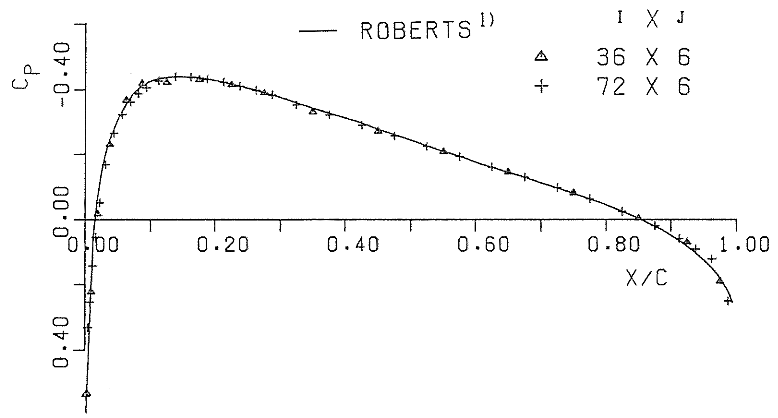

Fig. 7. Calculated chordwise distributions of pressure coefficient (I = number of panels per wing strip, J= number of wing strips per half wing, NACA 0015, $\alpha=0°$, $\eta=0.55$)

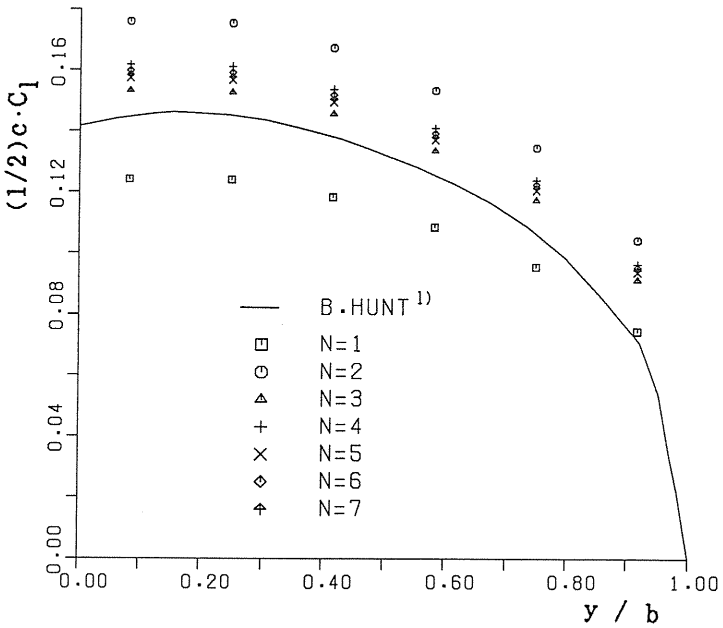

Fig. 8(*a*). Effect of multiplying factor *N* for chordwise discretization of doublet sheet on local lift (NACA 0005, $\alpha=5°$)

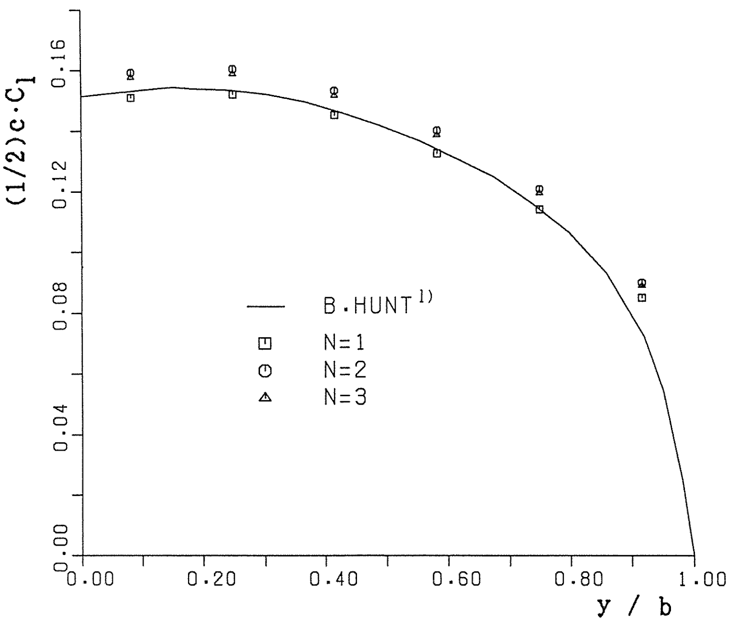

Fig. 8(*b*). Effect of multiplying factor *N* for chordwise discretization of doublet sheet on local lift (NACA 0015, $\alpha=5°$)

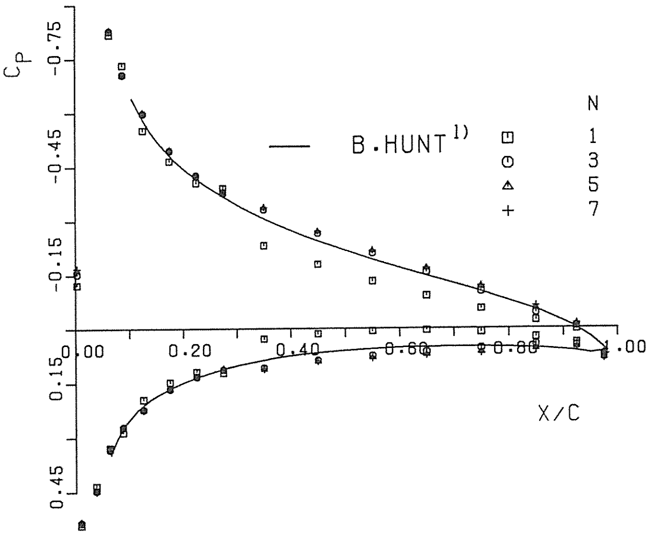

Fig. 9. Effect of multiplying factor N on chordwise distribution of pressure coefficient (NACA 0005, $\alpha=5°$, $\eta=0.60$)

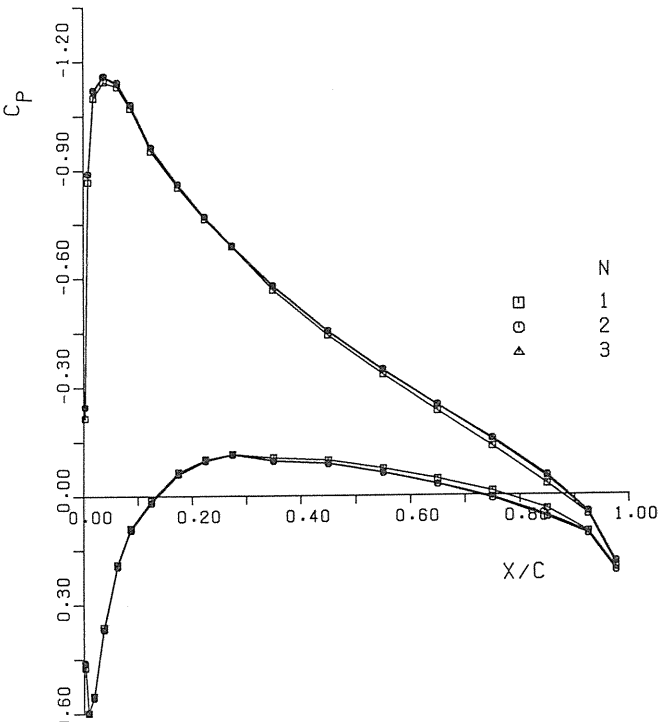

Fig. 10. Effect of multiplying factor N on chordwise distribution of pressure coefficient (NACA 0015, $\alpha=5°$, $\eta=0.58$)

The effect of the multiplying factor N on C_p is also shown in Figs. 9 and 10 for $t/c=0.05$ and 0.15 respectively. N means that a wing has N times as many number of doublet panels per wing strip as that of source panels per upper (or lower) wing strip. In the case of a thick wing, the curves of C_p distribution for various values of N do not show marked difference. For a thin wing of $t/c=0.05$, however, the lines of C_p distribution show some difference and become closer to the datum result as N becomes larger. Similar tendencies are observed for lift distribution $(1/2)c \cdot C_l$ from Figs. 8(*a*) and (*b*). The lift curve for $t/c=0.05$ approaches to the datum one of Hunt from a large value of $(1/2)c \cdot C_l$ as N increases. The converged result is about 8% larger than that of Hunt. It may be, therefore, asserted that it is possible to obtain better results with 'lines model' even for a thin wing, by increasing only the number of doublet panels per wing strip.

5. Conclusions

A computer code based on the 1st order panel method ('lines model') is presented for solving the incompressible potential flow around an airplane with an axisymmetric wing-body-tail configuration at an arbitrary angle of incidence in a uniform flow. An application of the code to a wing-only problem leads to the following conclusions.
(1) With no lift, it produces nearly accurate solution as that of higher order method, if with sufficient panels.
(2) With lift, the errors of computed results such as C_p and C_l tend to be larger as wing thickness becomes small, with the same number of panels.
(3) Better results may be obtained by increasing doublet panels only per wing strip, even for a thin wing, though not yet comparable to 'sheets model' results.

Nomenclature

A	=	coefficient matrix of linear equation system
$\boldsymbol{B}$	=	matrix whose i-th element is $\vec{n}_i \cdot \vec{V}_\infty / \lvert\vec{V}_\infty\rvert$
A_{ij}	=	influence coefficient, $\vec{n}_i \cdot \vec{C}_{ij}$
A/R	=	aspect ratio, $(2b)^2$/(wing area)
b	=	half span
c	=	local chord length
$\vec{C}_{ij}$	=	influence vector
C_p	=	pressure coefficient
C_d	=	local drag coefficient
C_l	=	local lift coefficient
$\vec{n}$	=	doublet's directional unit vector taken normally to doublet-distributed surface
N	=	multiplying factor for surface doublet discretization
$\vec{n}_p$	=	normal unit vector on point P of body surface
P	=	control (or collocation) point on which boundary condition is to be satisfied
Q	=	point on differential element dS *of* S
$\vec{r}$	=	vector drawn from Q to P
S	=	singularity-distributed surface
t	=	thickness of airfoil

$\vec{V}_\infty$	=	oncoming uniform velocity
X	=	solution column vector
x	=	coordinate established free-streamwise
y	=	coordinate established spanwise
Φ	=	total velocity potential
Ω	=	mathematical domain where harmonic function is defined
α	=	angle of incidence
μ	=	variable density per unit area of doublet distribution
σ	=	variable density per unit area of source distribution
$\phi(\xi)$	=	mode function of chordwise doublet distribution
μ_k	=	magnitude factor of doublet strip k
η	=	spanwise distance from axisymmetric plane normalized by half span, y/b
ξ	=	chordwise distance from leading edge normalized by local chord
∇^2	=	Laplacian operator
Γ	=	circulation or strength of line vortex

Subscript

i	control point
j	source-distributed panel
k	doublet-distributed wing strip
∞	undisturbed condition

References

1) Hunt, B., The panel method for subsonic aerodynamic flow, Computational Fluid Dynamics, Lecture Series 1978-4, von Karman Institute, 1980, pp.99–147.
2) Choi, J.S., A numerical analysis of incompressible potential flows around a sweptback wing by the panel method, Preprint of 24th Meeting of Chubu-Kansai Branch, Japan Soc. Aeronaut. Space Sci., 1987, pp. 97–100 (in Japanese).
3) Ballmann, J., Eppler, R. and Hackbusch, W., Panel methods in fluid mechanics with emphasis on aerodynamics; Note on numerical fluid mechanics, Vol. 21, Vieweg, 1988, pp. 1–34.

Appendix

Gaussian integral

Gauss' formula of approximate integration is written as follows,

for one variable;

$$\int_{-1}^{1} f(\xi)\,d\xi = \sum_k w_k \cdot f(\xi_k) \tag{a.1}$$

for two variables;

$$\int_{-1}^{1}\int_{-1}^{1} f(\xi,\eta)\,d\xi\,d\eta = \sum_j \sum_k w_j w_k f(\xi_j,\eta_k) \tag{a.2}$$

where w_j and w_k represent weight coefficients and ξ_j and η_k Gaussian points. These values can be get from the table. For the calculation of influence vector $\vec{C}_{ij}$ with Gauss' formula, the domain of integral needs to be transformed in such a way as shown Fig. A-1. The equations for coordinate transformation are

$$x_i = \sum_{n=1}^{4} F_n(\xi_i) x_{ni} \qquad (i=1,2) \tag{a.3}$$

where x_{ni} denotes i-coordinate of the n-th vertex of a plane panel before transformation (x,y coordinate of Fig. A-1), F_n's are interpolation functions expressed as follows (ξ_i is ξ,η of Fig. A-1),

$$\begin{aligned} F_1(\xi_i) &= (1/4)(1-\xi_1)(1-\xi_2) \\ F_2(\xi_i) &= (1/4)(1+\xi_1)(1-\xi_2) \\ F_3(\xi_i) &= (1/4)(1+\xi_1)(1+\xi_2) \\ F_4(\xi_i) &= (1/4)(1-\xi_1)(1+\xi_2) \end{aligned} \tag{a.4}$$

Thus, by the coordinate tranformation such as equation (a.4), the integral becomes:

$$\vec{C}_{ij} = \iint_{\substack{\text{panel}\\ j}} \vec{K} \mathrm{d}S = \int_{-1}^{1} \int_{-1}^{1} \vec{K} \,|\boldsymbol{J}|\, \mathrm{d}\xi \mathrm{d}\eta \tag{a.5}$$

where $\vec{K} = \vec{r}/r^3$ *and* $|\boldsymbol{J}|$ is the Jacobian determinant. Now with equation (a.2), the integration of equation (a.5) can be numerically calculated.

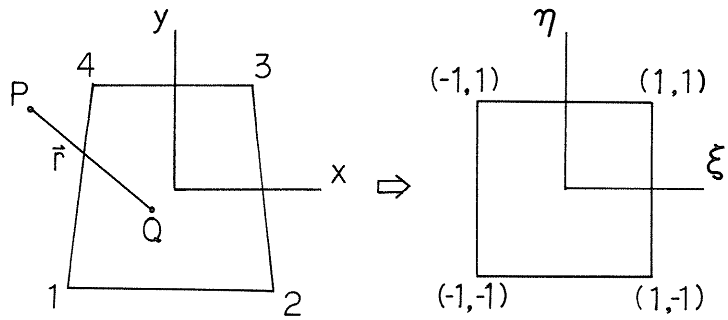

Fig. A-1. Transformation of integration domain